

## IN SITU STUDIES OF AQUEOUS CORROSION OF TARGET AND STRUCTURAL MATERIALS IN WATER IRRADIATED BY AN 800 MeV PROTON BEAM

Darryl P. Butt<sup>\*</sup>, Gary S. Kanner<sup>\*</sup>, Luke L. Daemen<sup>\*\*</sup>, Stuart Maloy<sup>\*</sup>, and R. Scott Lillard<sup>\*</sup>

<sup>\*</sup>Materials Science and Technology Division  
Materials Corrosion and Environmental Effects Laboratory  
and

<sup>\*\*</sup>Manuel Lujan Neutron Scattering Center  
Los Alamos National Laboratory  
Los Alamos, NM 87545 U.S.A.

### Abstract

Radiation enhanced, aqueous corrosion of solid neutron-targets such as tungsten or tantalum, or target cladding or structural materials such as superalloys and stainless steels, is a significant concern in a variety of accelerator systems and applications. In this paper we briefly describe our current methods for control and *in situ* monitoring of corrosion in accelerator cooling water loops. Using floating, electrochemical impedance spectroscopy (EIS), we have measured the corrosion rates of aluminum 6061, copper, Inconel 718, and 304L stainless steel in the flow loop of a water target irradiated by a milliamp, 800 MeV proton beam. Impedance spectroscopy allows us to model the corrosion process of a material as an equivalent electrical circuit. Thus, the polarization resistance, which is inversely proportional to the corrosion rate, can be extracted from the frequency response of a metal specimen. During a three month period of irradiation, without the use of corrosion mitigation techniques, we observed increases of several orders of magnitude in the water conductivity and the corrosion rates. The increase in corrosion is attributed to a build up of peroxide in our pseudo-closed loop system.

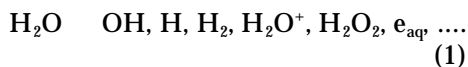
In addition, we monitored the conductivity by EIS and carried out solution analyses of water in a loop containing a bundle of tungsten rods. The rods were irradiated directly by the same 800 MeV beam. It was found that for a freshly purged system, the conductivity increased approximately two orders of magnitude in

one to a few days. Chemical analyses of the water in the loop showed the predominate ion to be tungsten. Using the tungsten ion concentrations, it was possible to calculate and correlate the theoretical conductivity with the measured conductivities. Thus, the change in conductivity was entirely attributable to tungsten dissolution. Consequently, we could estimate a non-conservative corrosion rate for the tungsten of 25 to 80  $\mu\text{m}/\text{year}$ .

In this paper we also briefly describe our second generation experiments, scheduled to begin in early 1997. In these experiments we plan to measure the corrosion rates of tungsten, tantalum, Inconel 718, 316L and 304L stainless steel, HT-9 ferritic martensitic stainless steel, and aluminum 5053 and 6061. Two or three electrode probes of each material are being placed directly in the proton beam, in a high neutron flux region, or a significant distance from the high radiation area. We will be measuring corrosion rates, changes in pH and conductivity, controlling hydrogen water chemistry, and we will be establishing parameters for filtration and mitigation of corrosion. We will also discuss our ideas for making *in situ* measurements of water radiolysis using optical and laser diagnostic techniques. Using such techniques it is possible to directly observe the production of corrosive radiolysis products as well as corrosion products near the surface of a target in a high energy particle beam.

### Introduction

It is well known, primarily from the wealth of experience with nuclear reactors, that radiation can significantly accelerate the aqueous corrosion of materials. In a radiation environment, elementary particles passing through water will lead to its radiolysis as follows:<sup>1</sup>



The majority of radiolysis products, or radicals, have lifetimes of milliseconds or less. The concentrations of some species,  $\text{H}_2\text{O}_2$  in particular, can build up to relatively high steady state concentrations. Both short lived and long lived radicals can lead to accelerated corrosion. In an accelerator environment, the short lived radicals are primarily a concern only when produced very near a metal surface, that is, a surface directly impinged by the high energy particle beam. As the beam travels through and radiolyzes water, it can produce concentrations of radicals along its track of the order 1-3 M.<sup>1</sup> The concentration of these species becomes vanishingly small just a short distance away from (or time beyond) the radiolysis event due to diffusion and recombination of these unstable and reactive species.

In addition to radiolysis products, radiation damage can affect the corrosion behavior of a material. In particular, elastic collisions between the incident, high energy particles and the nuclei of the material leads to large local atomic displacements which result in irreversible plastic deformation and heating. Generally this produces a material with a higher configurational free energy, which typically leads to more rapid corrosion. However, under certain conditions a higher free energy could lead to the rapid formation of a protective, passive oxide.

Thus, we have set out to develop techniques to both measure and directly observe the corrosion of materials in the radiation environments produced by a high energy particle beam. The techniques we are developing are aimed at understanding the corrosion of materials in or near the

path of a high energy beam as well as some distance away where only stable radiolysis products are important. A number of proof-of-concept experiments have been conducted this past year, and will be described below. In addition, we briefly describe a second series of experiments for which are currently preparing that will make use of more sophisticated diagnostics.

## Impedance Spectroscopy

Electrochemical Impedance Spectroscopy (EIS) was used to evaluate the corrosion of copper, aluminum 6061, Inconel 718, and 304L stainless steel in a pseudo-closed water loop, irradiated by an 800 MeV particle beam as illustrated schematically in Fig. 1. The particle beam passed through a so called degrader, consisting essentially of a complex network of water channels that served to maximize the time that the water spent in contact with the beam. Thus, the water leaving the degrader was highly radiolyzed. Because the system was pseudo-closed loop (meaning the rate of water added and removed from the system was small compared to the total system volume) it was anticipated that long lived radiolysis products, namely  $\text{H}_2\text{O}_2$ , would build up in the system until a steady state level was achieved. Corrosion cells were plumbed into the degrader loop both on the supply and return sides. The corrosion cells were shielded from direct radiation and were located approximately 5 meters above the degrader and so changes in corrosion were from changes in water chemistry not from radiation damage. Three three-electrode corrosion probes, as illustrated in Fig. 2, were inserted into each corrosion cell. These probes consisted of either one or two samples, or working electrodes, and one or two C-276 reference electrodes.

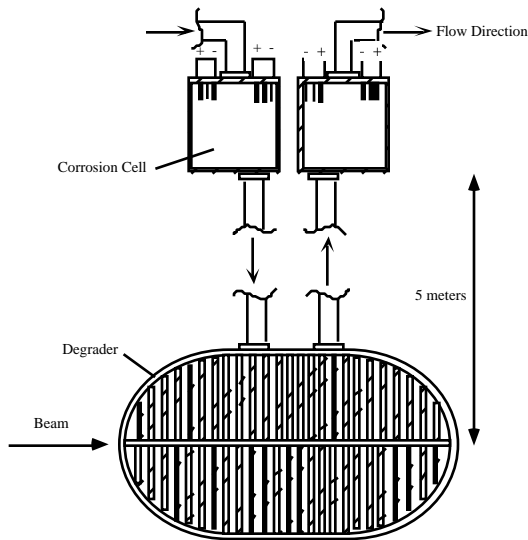


Fig. 1. Schematic illustration of the pseudo-closed loop flow system used to measure the effects of radiolyzed water on corrosion. Not drawn to scale.

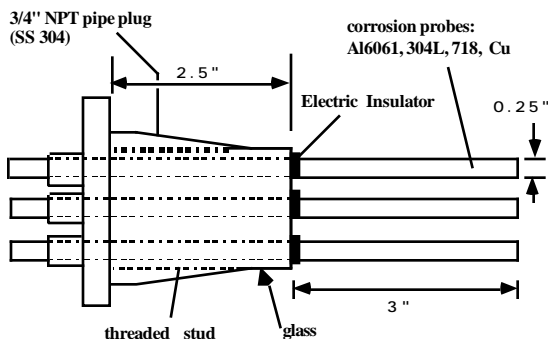


Fig. 2. Schematic illustration of a three-electrode corrosion probe.

Using floating EIS, we measured the time-dependent current response of the electrode surfaces to small sinusoidal, alternating potentials. Thus, by fitting the

data to equivalent electric circuit models, we could determine response variables such as corrosion rate (inversely proportional to polarization resistance), and solution conductivity (inversely proportional to geometric solution resistance). Fig. 3 shows an example of measurements made on 304L stainless steel on the return side of the degrader loop. The data are represented in this figure as both Bode magnitude (impedance,  $Z$ ) and Bode phase (phase shift,  $\theta$ ) plots. The corrosion rates and solution conductivities are thus calculated by determining the equivalent circuit components  $R_{pol}$  and  $R_{sol}$  shown in Fig. 3.

Equivalent circuit models, such as that illustrated in Fig. 3, were determined for each material in the closed loop system as a function of time. As shown in Figs. 4 and 5 below, during a three month period, without the use of corrosion mitigation techniques, we observed increases of several orders of magnitude in the water conductivity and the corrosion rates. We believe the increase in conductivity is at least partially due to a build up of peroxide and metal ions in our pseudo-closed loop system. The corrosion rates increased steadily due to the build up of peroxide, that is, cathodic reactants, the concentration of which had apparently not reached a steady state level by the end of this series of measurements. It is notable that over the course of two months, the corrosion rates of the four materials increased by one to four orders of magnitude due to the effects of radiolysis. Further details on these and other corrosion measurements have been reported elsewhere.<sup>2</sup>

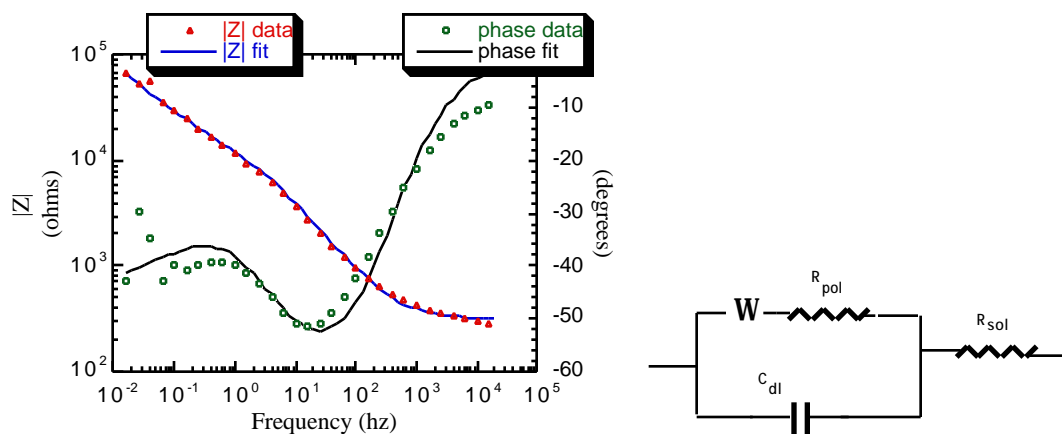


Fig. 3. EIS data and schematic of the corresponding equivalent circuit, obtained during a corrosion measurement taken on 304L stainless steel in a pseudo-closed loop flow system of a water target radiolyzed by an 800 MeV particle beam.  $W$  is the Warburg impedance (a diffusion term),  $R_{pol}$  is the polarization resistance (inversely proportional to corrosion current),  $R_{sol}$  is the solution resistance,  $C_{dl}$  is the double layer capacitance.

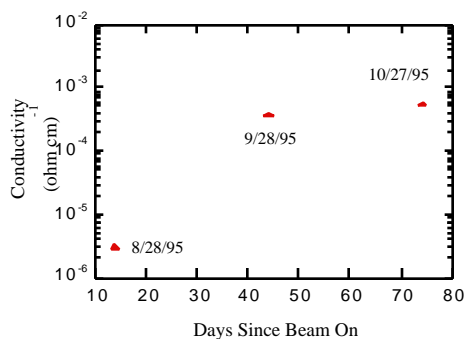


Fig. 4. Chronology of conductivity measurements made by EIS in the water target flow system.

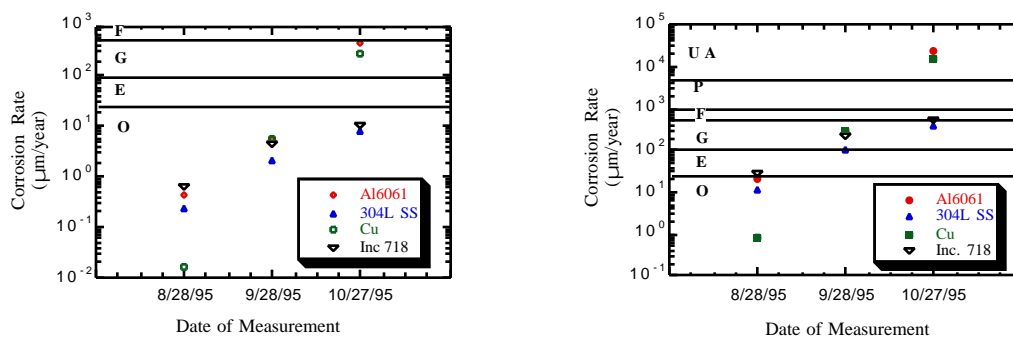


Fig. 5. Chronology of corrosion rates measured by EIS in the water target flow system: (a) shows the rates assuming uniform corrosion, and (b) shows the rates assuming pitting occurred over 2% of the surface area. The symbols O, E, G, F, P, and UA represent regions of corrosion considered to be outstanding, excellent, good, fair, poor, and unacceptable, respectively.

### Solution Conductivity Measurements in Tungsten Loop

Recently, we monitored the conductivity by EIS and carried out solution analyses of water in a closed loop containing a bundle of tungsten rods. Greater detail on these studies are being documented elsewhere and can be obtained from the authors.<sup>3</sup> The rods were irradiated directly by the same 800 MeV beam used to irradiate the degrader loop described above. As shown in Fig. 6, it was found that for a fresh system, the conductivity increased approximately two orders of magnitude, from  $10^{-6}$  to  $10^{-4}$  ohm<sup>-1</sup>cm<sup>-1</sup>, during the 150 hour exposure period. Chemical analyses of the water in the loop showed the predominate ion to be tungsten. Concentrations were on the order 30 µg/mL after 1 day of irradiation. Using the tungsten ion concentrations measured as a function of time (and at the same time conductivity measurements were made), it was possible calculate and correlate the theoretical resistivity (conductivity<sup>-1</sup>) with the measured resistivities as illustrated in Fig. 7. Thus, the change in conductivity was entirely attributable to tungsten dissolution. Consequently, we could estimate non-conservative corrosion rates for the tungsten assuming uniform corrosion. As illustrated in Fig. 8, the corrosion rates were on the order of 25 to 80 µm/year, which is a relatively rapid rate. It is likely that the actual, local rates of corrosion are much higher since the proton beam only impinges a small area on the bundle surface. It must be emphasized that in this particular system no effort was made to mitigate corrosion. In our second generation corrosion loop we plan to investigate mitigation strategies, for example, by controlling hydrogen water chemistry.

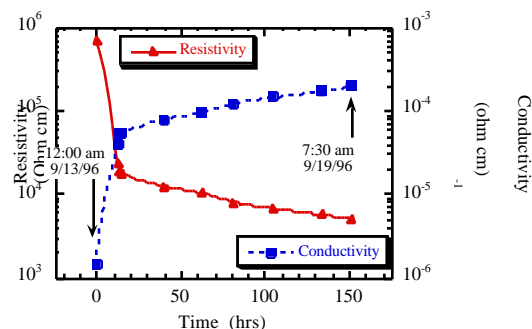


Figure 6. Solution resistivity and conductivity measured by EIS in a water loop containing a tungsten bundle irradiated by a milliamper 800 MeV proton beam.

In our second generation experiments we will measure, by EIS, the corrosion rates of tungsten, tantalum, Inconel 718, 316L and 304L stainless steel, HT-9, and aluminum 5053 and 6061. We have designed unique corrosion probes that will be placed directly in the high energy particle beam and in a region of high neutron flux. At this date, the probe designs are proprietary so can not be described in detail. However, they consist essentially of hollow, ceramic sealed tubes instrumented with internal thermocouples. Probes similar to that shown in Fig. 2 will be placed approximately 5 meters above the particle beam, as was done in the degrader loop experiments. In addition to measuring the corrosion rates and water conductivity, we will also monitor pH at several locations in the system using tungsten/tungsten oxide sensing electrodes which exhibit a Nernstian pH response.<sup>4</sup> In the course of these experiments we will also investigate the effects of scavengers, hydrogen in particular, on corrosion. It is well known, primarily from nuclear reactor experience, that hydrogen prevents the recombination of OH into H<sub>2</sub>O<sub>2</sub>, and thus reduces the levels of cathodic reactant.

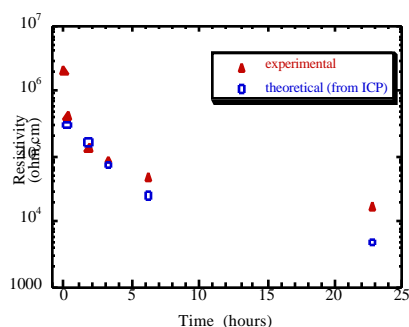


Figure 7. Measured versus theoretical resistivities obtained from a water loop containing a tungsten bundle irradiated by a milliamp 800 MeV proton beam. The experimental values were measured by EIS. The theoretical values were calculated from the measured concentrations of tungsten ions in solution.

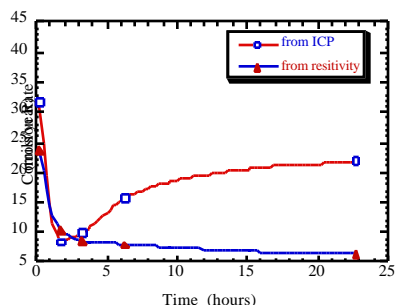


Figure 8. Calculated corrosion rates for tungsten in water during irradiation by a milliamp 800 MeV proton beam. These rates were calculated from measurements of resistivity and tungsten concentrations and in the water loop and assuming uniform corrosion. Thus, these are non-conservative estimates of the corrosion rate, which likely is locally more rapid in areas where the beam directly impinges on the metal surface.

### In Situ Diagnostics of Corrosion and Radiolysis Products

We currently use a machinable tungsten target in our accelerator at Los Alamos. Pure tungsten is also a candidate target for accelerator production of tritium. Therefore, we are particularly concerned

with the interaction of tungsten with water radiolysis products. In addition to the *in situ* corrosion measurements described above, we are working toward directly observing the interactions between tungsten and both short and long lived radiolysis products. Towards this end we are developing laser diagnostic methods that will allow us to identify a variety of reactant and product species in a high energy radiation environment. Currently, we are assimilating base line data for measuring the transient Raman spectra associated with reactive species generated by a high energy proton beam. For example, we have developed laser diagnostics that allow us to directly observe and, thus, correlate the decay of peroxide with the corrosion of tungsten as described below.

We have performed steady state Raman measurements on a tungsten plate immersed in dilute aqueous solutions of  $H_2O_2$  to study the effect of long-lived radiolysis products on corrosion. Before immersion, no Raman modes could be detected from the W surface. As shown in Fig. 9, after immersion, we observed Raman vibrational modes associated with soluble tungsten oxyhydroxides.<sup>5-7</sup> As these modes develop, the intensity of the O-O stretch ( $875\text{ cm}^{-1}$ ) of  $H_2O_2$  decreases, suggesting chemical reduction of  $H_2O_2$  and the corresponding corrosion of tungsten. As shown in Fig. 10, this observation is in agreement with electrochemical studies that we have performed on tungsten, which demonstrate that the corrosion rate increases with increasing concentrations of cathodic reactant, i.e.,  $H_2O_2$ . At the initial pH ( $4\pm0.5$ ), W is expected to form a passive oxide. Tungsten oxide ions or hydrates may also appear in solution, particularly under alkaline conditions.<sup>8</sup> The tungsten oxide vibrational mode at  $960\text{ cm}^{-1}$  shown in Fig. 9 is assigned to a terminal W=O stretch of a hydrated oxide molecule in an octahedral geometry<sup>5-7</sup>, whereas the band at  $550\text{ cm}^{-1}$  has been attributed to a symmetric stretch of a  $WO_2$  group.<sup>5,8</sup> These stretches were observed only in the solution and not on the tungsten surface. Thus, the tungsten is corroding by a dissolution mechanism as

was suspected in the conductivity experiments described above.

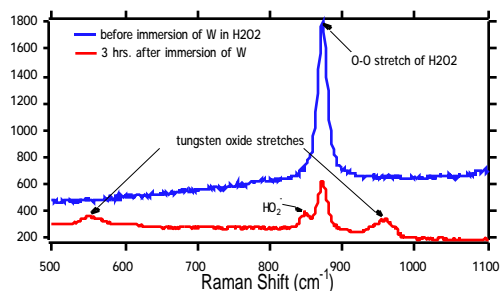


Fig. 9. Steady state measurement of corrosion of tungsten by hydrogen peroxide.

Another interesting result is the appearance of a mode associated with the O-O stretch of  $\text{HO}_2^-$ . For acidic pH the decomposition of  $\text{H}_2\text{O}_2$  should give rise to  $\text{O}_2$ ,  $\text{H}_2$ , or  $\text{H}_2\text{O}$ . However, after immersing W in the solution we observe the formation of a peak at  $849\text{ cm}^{-1}$ . We have verified that this peak is due to the peroxide ion by observing a shift of the O-O stretch frequency from  $875$  to  $849\text{ cm}^{-1}$  as the pH of the peroxide solution is changed from 4 to 13, where only the peroxide ion is stable. The  $\text{HO}_2^-$  peak disappears after 20 hours of immersion of tungsten, decomposing into  $\text{O}_2$ ,  $\text{H}^+$ , and 2 electrons. This result was consistent with a measured simultaneous decrease of the pH to below 2.

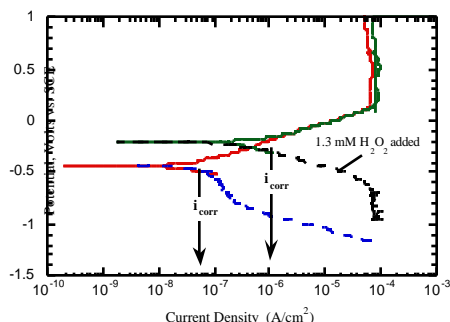


Fig. 10. Polarization curves for tungsten in 0.1 M NaCl, with and without the addition of peroxide. The corrosion rate (proportional to  $i_{\text{corr}}$ ) increases with increased cathodic reactant.

Recently, we have performed Raman spectroscopy on a 2 cm water cell that was irradiated for several hours by 800 MeV protons at a beam current of 500 nA. We calculated an expected concentration of  $\text{H}_2\text{O}_2$  under these conditions of about 20 mM. The intensity of a band at  $875\text{ cm}^{-1}$  in the Raman spectrum indicates that the actual concentration may have been as high as 140 mM. We are therefore checking the parameters in our calculations, and planning another series of radiolysis experiments to resolve this discrepancy.

The above results were obtained under nonresonant conditions ( $514.5\text{ nm}$  excitation), and with an instrument optimized for near infrared rather than visible detection. We believe that using resonant excitation, and UV-sensitive instruments, even smaller concentrations of reactive species and products could be detected.

## Acknowledgments

The authors are grateful for the assistance and advice of Ms. Doris Ford, Drs. Stuart Maloy, Walt Sommer, Robert Brown, and Eugene Zimmerman of Los Alamos National Laboratory, and Dr. Jay LaVerne of University of Notre Dame. This research was funded by the U.S. Department of Energy.

## References

1. A. V. Byalobzheskii, *Radiation Corrosion*, TT 70-50005, AEC-tr 7096, U.S. Atomic Energy Commission and the National Science Foundation, Washington, D.C. 1970.
2. R. S. Lillard and D. P. Butt, *Preliminary Spallation Neutron Source Corrosion Experiments: Corrosion Rates of Engineering Materials in a Water Degraded Cooling Water Loop Irradiated by an 800 MeV Proton Beam*, Los Alamos National Laboratory Report, LAUR 96-1011, 1996.
3. R. S. Lillard, D. P. Butt, S. Maloy, and W. Sommer, *Materials Corrosion and Mitigation Strategies for APT: Using Solution Resistivity as an Estimate of Tungsten Corrosion in Spallation Neutron Target Cooling Loops*, to be submitted as an

unclassified Los Alamos National Laboratory Report.

4. L. B. Kriksunov, D. D. Macdonald, and P. J. Millett, *J. Electrochem. Soc.*, **141** [11] 3002 (1994).

5. B. Soptrajanov, A. Nikolovski, and I. Petrov, *Spectrochimica Acta*, **24A**, 1617 (1968).

6. M. F. Daniel, B. Desbat, J. C. Lassegues, B. Gerand, and M. Figlarz, *J. Solid State Chem.*, **67**, 235 (1987).

7. D. S. Kim, M. Ostromecki, I. E. Wachs, S. D. Kohler, and J. G. Ekerdt, *Catalysis Lett.*, **33**, 209 (1995).

8. M. Pourbaix, *Atlas of Electrochemical Equilibria*, pp 280-285, NACE, Houston, TX, 1974.

9. C. Aubry, G. Chottard, N. Platzner, J. M. Bregeault, R. Thouvenot, F. Chauveau, C. Huet, and H. Ledon, *Inorg. Chem.*, **30** [23] 4409 (1991).